

Tuning electronic properties of $\text{FeSe}_{0.5}\text{Te}_{0.5}$ thin flakes by a novel field effect transistor

C. S. Zhu^{1,†}, J. H. Cui^{1,†}, B. Lei¹, N. Z. Wang¹, C. Shang¹, F. B. Meng¹,
L. K. Ma¹, X. G. Luo^{1,4}, T. Wu^{1,4}, Z. Sun^{2,4}, and X. H. Chen^{1,3,4*}

¹*Hefei National Laboratory for Physical Sciences at Microscale and Department of Physics,
and CAS Key Laboratory of Strongly-coupled Quantum Matter Physics,
University of Science and Technology of China, Hefei, Anhui 230026, China*

²*National Synchrotron Radiation Laboratory, University of Science and Technology of China, Hefei, Anhui 230026, China*

³*High Magnetic Field Laboratory, Chinese Academy of Sciences, Hefei, Anhui 230031, China*

⁴*Collaborative Innovation Center of Advanced Microstructures, Nanjing University, Nanjing 210093, China*

(Dated: September 5, 2018)

Using a field-effect transistor (FET) configuration with solid Li-ion conductor (SIC) as gate dielectric, we have successfully tuned carrier density in $\text{FeSe}_{0.5}\text{Te}_{0.5}$ thin flakes, and the electronic phase diagram has been mapped out. It is found that electron doping controlled by SIC-FET leads to a suppression of the superconducting phase, and eventually gives rise to an insulating state in $\text{FeSe}_{0.5}\text{Te}_{0.5}$. During the gating process, the (001) peak in XRD patterns stays at the same position and no new diffraction peak emerges, indicating no evident Li^+ ions intercalation into the $\text{FeSe}_{0.5}\text{Te}_{0.5}$. It indicates that a systematic change of electronic properties in $\text{FeSe}_{0.5}\text{Te}_{0.5}$ arises from the electrostatic doping induced by the accumulation of Li^+ ions at the interface between $\text{FeSe}_{0.5}\text{Te}_{0.5}$ and solid ion conductor in the devices. It is striking that these findings are drastically different from the observation in FeSe thin flakes using the same SIC-FET, in which T_c is enhanced from 8 K to larger than 40 K, then the system goes into an insulating phase accompanied by structural transitions.

PACS numbers: 74.25.F-, 74.70.Xa, 74.78.-w

Tuning carrier concentration is one of the most powerful approaches in the condensed matter physics for the explorations of novel quantum phases and exotic electronic properties as well as their underlying physical mechanics [1–8]. To overcome the inherent doping limit in the material synthetic methods, field effect transistor (FET) configurations have been applied to tune material properties using gating by electric field [9]. Two types of FET, metal-insulator-semiconductor (MIS) FET and electric double layer (EDL) FET, are widely used to control the charge carrier density on the surface of materials [10, 11]. In order to change the carrier density in the bulk, the so-called ionic field-effect transistor (iFET) with gel-like electrolyte as the gate medium has been used to drive Li^+ ions into layered materials. This type of FET configuration can effectively modulate 1T-TaS₂ electronic properties by the tunable Li^+ ion intercalation [12]. However, the heavily-doped electronic states in all these FET configurations are confined at the interfaces or overlaid with electrolyte, which prevents them from being characterized by many physical measurements. On the other hand, conventional MIS-FET devices cannot provide sufficient carriers to induce novel phases, such as superconductivity, by electrostatic doping, and the liquid or gel-like electrolyte is not compatible with modern solid electronics and may react with samples when gating voltage is applied [11, 13, 14]. Recently, we have fabri-

cated a new type of FET device (see Fig. 1(c)) using solid ion conductor (SIC) as a gate dielectric. This type of FET configuration overcomes the inherent limitations mentioned above, and its application on FeSe thin flakes reveals some substantial advantages of the SIC-FET [15].

Using the SIC-FET devices, we are able to tune the carrier density of FeSe by driving lithium ions in and out of the FeSe thin flakes and thus control the material properties and its phase transitions. With the intercalation of Li^+ ions, new structural changes have been identified by *in-situ* XRD measurements. A wide carrier-doping phase diagram has also been mapped out with increasing Li^+ content. A dome-shaped superconductivity with maximal T_c above 40 K was obtained and an insulating phase was reached at extremely overdoped regime. In addition, we have demonstrated that many experimental probes can be applied to uncover novel structural phases that are inaccessible in ordinary conditions [15]. The application of such a novel FET device can provide exciting opportunities for exploring new quantum phases and novel materials.

FeTe and FeSe share the same crystal structure. The former has very strong electron correlation, while the latter shows only moderate electron correlation [16]. The isovalent substitution of Te for Se results in a remarkable change of electron correlation [16, 17]. Transport measurements have shown that, upon substitution, T_c increases from 8 K in FeSe to the maximum of ~ 14 K around $x \sim 0.5$ in $\text{FeSe}_{1-x}\text{Te}_x$, and bulk superconductivity disappears for $x > 0.7$ [18–23]. In FeSe and its derived compounds, T_c can be significantly increased up to more

[†] These authors contributed equally to this work.

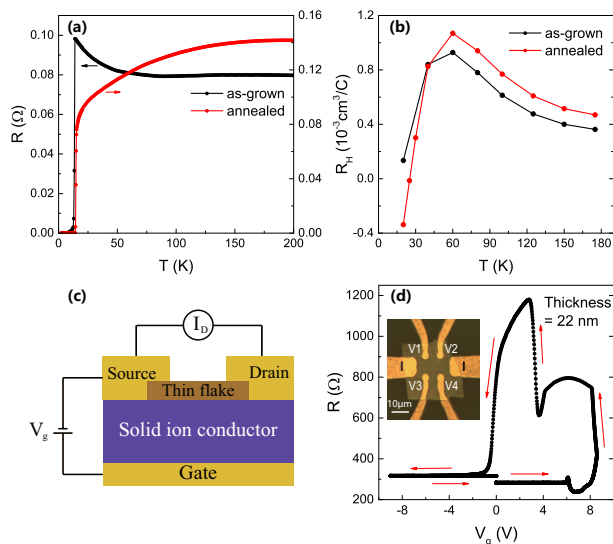


FIG. 1: (color online). (a): Temperature-dependent resistivity of as-grown and O_2 -annealed $FeSe_{0.5}Te_{0.5}$ bulk single crystals. (b): Temperature-dependent Hall coefficient R_H of as-grown and O_2 -annealed $FeSe_{0.5}Te_{0.5}$ thin flakes. (c): A schematic plot of the SIC-FET device with the solid ion conductor as the gate dielectric. (d): A gate-voltage dependence of the resistance of $FeSe_{0.5}Te_{0.5}$ thin flakes with thickness of 22 nm. The insert is the optical image of a $FeSe_{0.5}Te_{0.5}$ thin flake with the current and voltage terminals labeled.

than 40 K when electron carriers are introduced into the bulk [24, 25]. On the basis of our previous studies on FeSe thin flakes, it is interesting to investigate whether the T_c of $FeSe_{1-x}Te_x$ can also be significantly improved by introduction of electronic carrier using the same SIC-FET approach and how the enhanced electron correlation with Te doping influences the superconductivity.

In this paper, we use the SIC-FET device to investigate how electron doping can modify the electronic properties of $FeSe_{0.5}Te_{0.5}$. In contrast to the case of FeSe [15], we found that Li^+ intercalation is not evident in $FeSe_{0.5}Te_{0.5}$ and that there is no structural transition during the gating process. However, the electronic properties can still be modulated, suggesting that Li^+ ions accumulate at the interface between the thin flake and the SIC substrate and induce electrostatic doping in $FeSe_{0.5}Te_{0.5}$. Though electron-type carriers are doped into $FeSe_{0.5}Te_{0.5}$ system, Hall measurements indicate that hole-type carriers always dominate the transport properties at high temperatures. With increasing the gate voltage, the superconducting state is suppressed, and eventually an insulating phase emerges, which could be related to the strong electron correlation in $FeSe_{0.5}Te_{0.5}$. These findings are strikingly different from the observation of FeSe thin flakes using the same SIC-FET device, in which the T_c can be enhanced from 8 K (low T_c phase) to more than 40 K (high T_c phase).

The as-grown $FeSe_{0.5}Te_{0.5}$ crystals are superconduct-

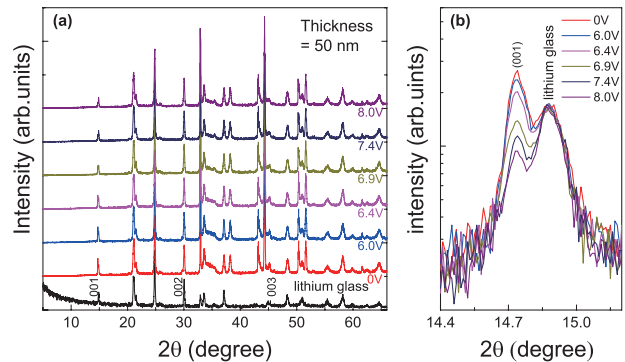


FIG. 2: (color online). (a) The typical *in-situ* XRD patterns of the $FeSe_{0.5}Te_{0.5}$ thin flakes with thickness of 50 nm at various gating status. (b) The magnified view of the (001) diffraction peak.

ing and reach zero-resistance at $T = 11$ K (Fig. 1(a)). The non-metallic characteristic is caused by the localization effect from interstitial Fe [26, 27]. After removing the interstitial Fe by annealing crystals in oxygen, we improved the quality and enhanced the T_c^{zero} to 14.2 K. In Fig. 1(b), R_H shows a sign reversal below 30K in the annealed crystals, suggesting that electron-type carriers become intrinsically dominant at low temperatures. Using the annealed crystals and following the details as described in ref. [15], we fabricated SIC-FET devices, and performed resistance, Hall coefficient, and *in-situ* XRD measurements.

Figure 1(c) shows a schematic plot of the SIC-FET device we used to tune the electronic properties of $FeSe_{0.5}Te_{0.5}$ thin flakes. Using the solid state lithium ion conductive glass ceramics as the gate dielectric, we prepared devices with a standard Hall bar configuration (inset of Fig. 1(d)). Thin flakes with a typical thickness of 22 nm serve as the transport channel. Li^+ in the lithium ion conductor can be driven by electric field. With a positive gate voltage applied, Li^+ accumulates at the bottom of $FeSe_{0.5}Te_{0.5}$ thin flakes. As will be shown later, our XRD data and transport measurements suggest that Li^+ intercalation is minimal with further increasing the gate voltage. However, the electronic properties of $FeSe_{0.5}Te_{0.5}$ can still be drastically modulated by gating.

Figure 1(d) shows a typical $R-V_g$ curve taken at $T = 260$ K. The resistance of the $FeSe_{0.5}Te_{0.5}$ thin flake stays at the same value when $V_g < 5$ V. With increasing V_g above 5 V, the resistance varies and the details will be shown in Fig. 3. As the gate voltage is sweeping back, the resistance increases drastically by a factor of 4 and drops drastically when the gate voltage is descending to 0 V. Eventually it returns to a value close to its initial status with negative voltage applied. This behavior indicates that the modulation of electronic properties by gating is reversible. The slight different resistance of $FeSe_{0.5}Te_{0.5}$ before and after gating may arise from the degradation

of the bottom surface of thin flakes.

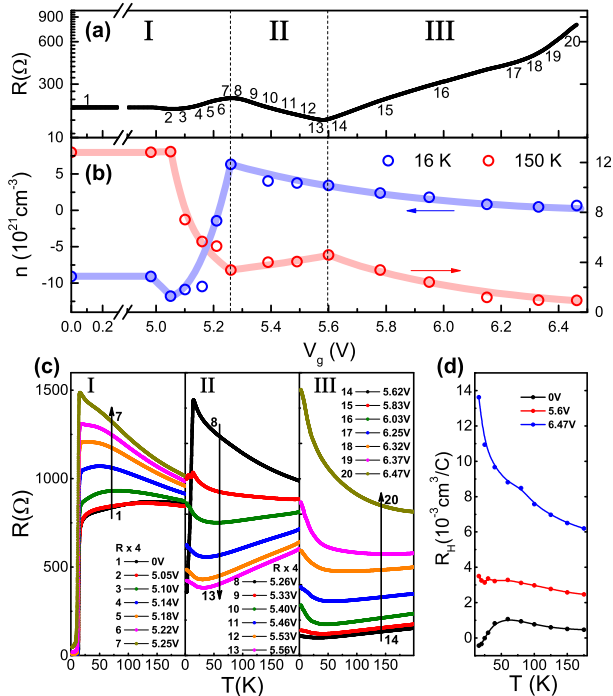


FIG. 3: (color online). (a): Gate voltage dependence of the resistance of a $\text{FeSe}_{0.5}\text{Te}_{0.5}$ thin flake with a thickness of 22 nm. (b): Hall number n_H with various gate voltage applied, taken at $T = 16$ K and 150 K. The low temperature n_H shows a sudden sign reversal around $V_g = 5.22$ V. (c): The longitudinal resistance at various gating status. (d): Temperature dependence of Hall coefficient R_H , calculated from the linear fit of a $R_{xy}(B)$ plot from -9 to 9 T. For the nonlinear $R_{xy}(B)$ curves, R_H was extracted from the slope of the high-field quasilinear part [15].

By performing *in-situ* XRD measurements on $\text{FeSe}_{0.5}\text{Te}_{0.5}$ devices, we studied whether the structure changes during the gating process. The 22 nm thin flakes are too thin to yield detectable signals, and we thus selected 50 nm $\text{FeSe}_{0.5}\text{Te}_{0.5}$ thin flakes for XRD characterization. Fig. 2(a) shows the typical XRD patterns at different charge stages. The (001) diffraction peak stays at the same position with increasing gate voltage (Fig. 2(b)), indicating that the interlayer separation is not affected by gating and that Li^+ intercalation should be minimal if it does occur. This behavior is different from FeSe thin flakes, in which Li^+ intercalation is substantial and causes structural transitions. The decrease of the (001) peak intensity could be attributed to the degradation of $\text{FeSe}_{0.5}\text{Te}_{0.5}$ bottom layer due to Li^+ accumulation, which can weaken the diffraction signals.

Though Li^+ intercalation is restrained, the accumulation of Li^+ ions at the interface can also cause electrostatic doping in $\text{FeSe}_{0.5}\text{Te}_{0.5}$ thin flakes. Fig. 3(a) shows the details of the evolution of resistance with gate voltage. The variation of resistance changes slightly for

different devices, while the dip-peak-valley feature and the rise of resistance at higher gate voltages are highly reproducible. To further demonstrate carrier doping, we performed Hall measurements. In Fig. 3(b), the Hall number $n_H = 1/eR_H$ measured at $T = 150$ K and $T = 16$ K varies drastically, suggesting that the carrier concentration in the bulk is strongly affected during gating. Based on the transport measurements, we empirically divide the charge doping process into three regions I, II and III, and plot the temperature-dependent resistance in Fig. 3(c). In the I region, the thin flakes show superconducting behavior, and the T_c is slightly suppressed with increasing the gate voltage. In this region, the corresponding low-temperature Hall number is negative, indicating that electron carriers are crucial for superconductivity. In the II region, the superconductivity is quickly suppressed and a semiconducting-like feature appears at low temperature. Above 30 K, from I to III region, the overall normal-state resistance increases, decreases and increases again, accompanied by several crossovers between metallic and semiconducting-like behavior.

Figure 3(d) plots the temperature dependence of the Hall coefficient R_H with different gate voltages. Except for the sign reversal behavior at low temperature in the I region, the transport properties of $\text{FeSe}_{0.5}\text{Te}_{0.5}$ are dominated by hole-type carriers. The overall R_H value rises strongly with increasing the gate voltage, indicating that electron doping in the thin flake is induced by gating to counteract the contribution from the hole-type carriers, though Fig. 3(b) shows that the behavior in the II region appears slightly anomaly at $T=150$ K. Generally speaking, as shown in our studies on FeSe thin flakes, Li^+ intercalation can bring a great amount of electrons into the system, however the Hall number in the II and III regions indicates that the hole carriers are always dominant in the gating range we studied here. These results serve as a clear evidence that Li^+ intercalation is minimal in our devices and cannot dope enough electrons.

Based on the resistance measurements, we plot an electronic phase diagram as a function of gate voltage for $\text{FeSe}_{0.5}\text{Te}_{0.5}$ (see Fig. 4(a)). The electronic phase diagram of FeSe is also shown for comparison (Fig. 4(b)). In $\text{FeSe}_{0.5}\text{Te}_{0.5}$, as V_g increases, a series of variations from superconducting phase to insulating phase take place. The evolution from superconductor to insulator induced by electron doping shares similar behavior with FeSe thin flakes. Nevertheless, one may notice two remarkable differences between $\text{FeSe}_{0.5}\text{Te}_{0.5}$ and FeSe. First, Li^+ ions can be easily intercalated into FeSe thin flakes, and consequently structural phase transitions have been observed [15]. However, Li^+ intercalation is minimal in $\text{FeSe}_{0.5}\text{Te}_{0.5}$ and there is no evident change in structure. This difference suggests that the substitution of Te for Se significantly changes the characteristics of two-dimensional FeSe layers and restrains the intercalation of Li^+ ions. Secondly, electron doping can drastically in-

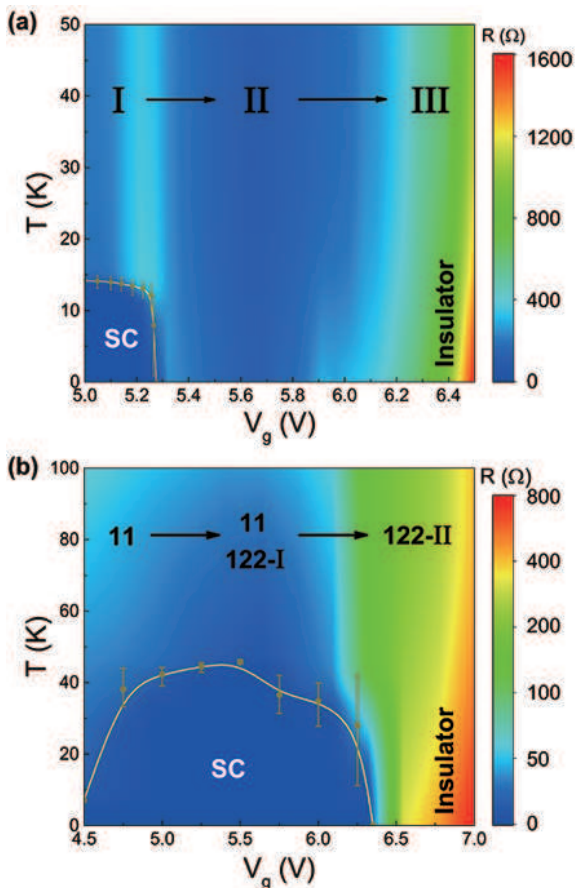


FIG. 4: (color online). (a): The phase diagram of $\text{FeSe}_{0.5}\text{Te}_{0.5}$ thin flake as a function of gate voltage. (b): The phase diagram of Li-intercalated FeSe thin flake as a function of gate voltage, and the data was taken from Ref. 15.

crease the T_c from ~ 8 K to more than 40 K for FeSe [15], but suppresses the T_c from ~ 14 K down to lower value instead of enhancing it for $\text{FeSe}_{0.5}\text{Te}_{0.5}$. This contrast suggests that the substitution of Te for Se severely changes the electronic properties, though the crystal structures of these two compounds are highly similar to each other.

Direct probing electronic structures by angle-resolved photoemission spectroscopy (ARPES) has shown that FeSe possesses moderate electron correlation with well-defined electronic bands, while the bands in $\text{FeSe}_{1-x}\text{Te}_x$ are heavily renormalized for $x \geq 0.5$, indicating strong electron correlation in this substitution region [16, 17]. This difference is likely responsible for the discrepancy of carrier doping-induced electronic properties in these two materials. The pristine FeSe has both of electron and hole pockets at the Fermi level with a relatively low T_c of 8 K. With heavy electron doping, the Fermi level shifts up drastically and electron pockets expand, the resultant electronic system shows a very high T_c more than 40 K. ARPES measurements of $\text{FeSe}_{0.5}\text{Te}_{0.5}$ show unambiguous hole pockets around the zone center Γ in k -space, while the electron pocket around the zone cor-

ner M is ill-defined. This characteristic explains why the hole-type carriers dominate significantly in Hall measurements at high temperatures. A detailed analysis of the ill-defined electron pockets suggests that the coherent spectral weight gradually increases as temperature is decreasing [28], which is naturally related to the sign reversal of Hall n_H at low temperatures. In $\text{FeSe}_{0.5}\text{Te}_{0.5}$, our data suggests that Li^+ intercalation is not evident and thus the electron doping is not so strong as the case in FeSe . Therefore, the consequent electronic structures after gating are remarkably different in FeSe and $\text{FeSe}_{0.5}\text{Te}_{0.5}$. This characteristic is consistent with the fact that hole-type carriers still contribute significantly to transport properties as high gate voltage is applied.

In Fig. 3(b), the high-temperature Hall data in the I region indicates that the electron doping can effectively counteract the hole-type carriers in transport properties. However, the evolution of Hall n_H at 16 K suggests that the contribution from electron-type carriers is also suppressed by electron doping. This anomalous trend is inconsistent with a rigid band model, in which electron doping is expected to increase electron-type carriers. We argue that such an anomaly should be associated with some novel change of electron pockets around M, in which a gap or a strong suppression of spectral weight may occur due to the increase of electron doping and results in a reduction of electron-type contribution in Hall n_H . With increasing the gate voltage, eventually both of electron-type and hole type carriers are suppressed and the whole system shows an insulating behavior. If we reverse the carrier doping procedure from the insulating phase, the evolution of the electronics states will show that a practical hole doping leads to superconductivity. Such a behavior shares similarity with cuprates, in which the superconductivity is realized by doping holes into a Mott insulator. From this perspective, we argue that there is novel physics of strong electron correlation during the change of electronic properties induced by gating. Further investigations of the transitions between different phases will enrich our understanding of the relationship between the superconductivity and the correlated electron state in the insulating region.

In summary, we have successfully modulated electronic properties of $\text{FeSe}_{0.5}\text{Te}_{0.5}$ thin flakes using SIC-FET configuration. Contrary to our previous studies of FeSe thin flakes, XRD patterns indicate that Li^+ intercalation is not evident in our $\text{FeSe}_{0.5}\text{Te}_{0.5}$ FET devices. Our data suggests that, Li^+ ions likely accumulate with the gate voltage applied at the interface between $\text{FeSe}_{0.5}\text{Te}_{0.5}$ and solid ion conductor, which can lead to electrostatic doping and is responsible for the drastic change of electronic properties of $\text{FeSe}_{0.5}\text{Te}_{0.5}$. A systematic variation of transport properties in $\text{FeSe}_{0.5}\text{Te}_{0.5}$ reveals a change of electronic states from a superconducting state to an insulating state, which can be related to the strong electron correlation in this material. The substitution

of Te for Se significantly changes the characteristics of two-dimensional FeSe layers, and enhances the electronic correlation.

This work is supported by the National Natural Science Foundation of China (Grants No. 11190021, No. 11534010 and No. 91422303), the Strategic Priority Research Program (B) of the Chinese Academy of Sciences (Grant No. XDB04040100), the National Key R&D Program of the MOST of China (Grant No. 2016YFA0300201), and the Hefei Science Center CAS (2016HSC-IU001).

* Electronic address: chenxh@ustc.edu.cn

- [1] A. D. Caviglia, S. Gariglio, N. Reyren, D. Jaccard, T. Schneider, M. Gabay, S. Thiel, G. Hammerl, J. Mannhart, and J.-M. Triscone, *Nature* **456**, 624-627 (2008).
- [2] K. Ueno, S. Nakamura, H. Shimotani, A. Ohtomo, N. Kimura, T. Nojima, H. Aoki, Y. Iwasa, and M. Kawasaki, *Nat. Mater.* **7**, 855-858 (2008).
- [3] K. Ueno, S. Nakamura, H. Shimotani, H. T. Yuan, N. Kimura, T. Nojima, H. Aoki, Y. Iwasa, and M. Kawasaki, *Nat. Nanotechnol.* **6**, 408-412 (2011).
- [4] J. T. Ye, S. Inoue, K. Kobayashi, Y. Kasahara, H. T. Yuan, H. Shimotani, and Y. Iwasa, *Nat. Mater.* **9**, 125-128 (2010).
- [5] A. T. Bollinger, G. Dubuis, J. Yoon, D. Pavuna, J. Misewich, and I. Bozovic, *Nature* **472**, 458-460 (2011).
- [6] Y. Saito, Y. Kasahara, J. T. Ye, Y. Iwasa, and T. Nojima, *Science* **350**, 409-413 (2015).
- [7] L. J. Li, E. C. T. O'Farrell, K. P. Loh, G. Eda, B. Ozyilmaz, and A. H. Castro Neto, *Nature* **529**, 185-189 (2016).
- [8] B. Lei, Z. J. Xiang, X. F. Lu, N. Z. Wang, J. R. Chang, C. Shang, A. M. Zhang, Q. M. Zhang, X. G. Luo, T. Wu, Z. Sun, and X. H. Chen, *Phys. Rev. B* **93**, 060501(R) (2016).
- [9] C. H. Ahn, S. Gariglio, P. Paruch, T. Tybell, L. Antognazza, and J.-M. Triscone, *Science* **284**, 1152-1155 (1999).
- [10] C. H. Ahn, A. Bhattacharya, M. Di Ventura, J. N. Eckstein, C. Daniel Frisbie, M. E. Gershenson, A. M. Goldman, I. H. Inoue, J. Mannhart, and J. Triscone, *Rev. Mod. Phys.* **78**, 1185-1212 (2006).
- [11] K. Ueno, H. Shimotani, H. T. Yuan, J. T. Ye, M. Kawasaki, and Y. Iwasa, *J. Phys. Soc. Jap.* **83**, 032001 (2014).
- [12] Y. J. Yu, F. Y. Yang, X. F. Lu, Y. J. Yan, Y. H. Cho, L. G. Ma, X. H. Niu, S. Kim, X. H. Chen, and Y. B. Zhang, *Nat. Nanotechnol.* **10**, 270-276 (2015).
- [13] J. Jeong, N. Aetukuri, T. Graf, T. D. Schladt, M. G. Samant, and S. S. P. Parkin, *Science* **339**, 1402-1405 (2013).
- [14] T. D. Schladt, T. Graf, N. B. Aetukuri, M. Y. Li, A. Fantini, X. Jiang, M. G. Samant, and S. S. P. Parkin, *ACS Nano* **7**, 8074-8081 (2013).
- [15] B. Lei, N. Z. Wang, C. Shang, F. B. Meng, L. K. Ma, X. G. Luo, T. Wu, Z. Sun, Y. B. Zhang, and X. H. Chen, arXiv:1609.07726.
- [16] A. Tamai, A. Y. Ganin, E. Rozbicki, J. Bacsá, W. Meevasana, P. D. C. King, M. Caffio, R. Schaub, S. Margadonna, K. Prassides, M. J. Rosseinsky, and F. Baumberger, *Phys. Rev. Lett.* **104**, 097002 (2010).
- [17] E. Ieki, K. Nakayama, Y. Miyata, T. Sato, H. Miao, N. Xu, X.-P. Wang, P. Zhang, T. Qian, P. Richard, Z. J. Xu, J. S. Wen, G. D. Gu, H. Q. Luo, H. H. Wen, H. Ding, and T. Takahashi, *Phys. Rev. B* **89**, 140506(R) (2014).
- [18] R. Khasanov, M. Bendele, A. Amato, P. Babkevich, A. T. Boothroyd, A. Cervellino, K. Conder, S. N. Gvasaliya, H. Keller, H.-H. Klauss, H. Luetkens, V. Pomjakushin, E. Pomjakushina, and B. Roessli, *Phys. Rev. B* **80**, 140511(R) (2009).
- [19] M. Bendele, S. Weyeneth, R. Puzniak, A. Maisuradze, E. Pomjakushina, K. Conder, V. Pomjakushin, H. Luetkens, S. Katrych, A. Wisniewski, R. Khasanov, and H. Keller, *Phys. Rev. B* **81**, 224520 (2010).
- [20] V. Tsurkan, J. Deisenhofer, A. Gunther, Ch. Kant, M. Klemm, H.-A. Krug von Nidda, F. Schrettle, and A. Loidl, *Eur. Phys. J. B* **79**, 289-299 (2011).
- [21] D. J. Gawryluk, J. Fink-Finowicki, A. Wisniewski, R. Puzniak, V. Domukhovski, R. Diduszko, M. Kozowski and M. Berkowski, *Supercond. Sci. Technol.* **24**, 065011 (2011).
- [22] C. H. Wu, W. C. Chang, J. T. Jeng, M. J. Wang, Y. S. Li, H. H. Chang, and M. K. Wu, *Appl. Phys. Lett.* **102**, 222602 (2013).
- [23] M. Bendele, Z. Guguchia, F. von Rohr, T. Irifune, T. Shinmei, I. Kantor, S. Pascarelli, B. Joseph, and C. Marini, *Phys. Rev. B* **90**, 174505 (2014).
- [24] B. Lei, J. H. Cui, Z. J. Xiang, C. Shang, N. Z. Wang, G. J. Ye, X. G. Luo, T. Wu, Z. Sun, and X. H. Chen, *Phys. Rev. Lett.* **116**, 077002 (2016).
- [25] J. G. Guo, S. F. Jin, G. Wang, S. C. Wang, K. X. Zhu, T. T. Zhou, M. He, and X. L. Chen, *Phys. Rev. B* **82**, 180520(R) (2010).
- [26] Y. Sun, T. Yamada, S. Pyon, and T. Tamegai, *Sic. Rep.* **6**, 32290 (2016).
- [27] Y. Sun, Y. Tsuchiya, T. Taen, T. Yamada, S. Pyon, A. Sugimoto, T. Ekino, Z. X. Shi, and T. Tamegai, *Sci. Rep.* **4**, 4585 (2014).
- [28] P. H. Lin, Y. Texier, A. Taleb-Ibrahimi, P. LeFevre, F. Bertran, E. Giannini, M. Grioni, and V. Brouet, *Phys. Rev. Lett.* **111**, 217002 (2013).